# Computation of Supersonic Turbulent Shear Layer Mixing with Mild Compressibility Effects

Dale K. Ota* and Uriel C. Goldberg*
*Rockwell International Science Center, Thousand Oaks, California 91360*

**Turbulent supersonic shear layer mixing has been computed using the USA-series multizone Reynolds-averaged Navier-Stokes solver, which is based on an implicit finite-volume total variation diminishing (TVD) formulation for the convection terms. Three shear layer cases were run using three turbulence models each: 1) algebraic, 2) one-equation $k - L$, and 3) two-equation $k - \varepsilon$. The results using the one- and two-equation models match experimental $U$-velocity profiles better than those using the algebraic model. Shear layer thickness and shear layer spreading rate predictions, using the $k - \varepsilon$ model, compare well with experimental data. Space-marched and time-marched calculations are found to produce practically the same results.**

## I. Introduction

SHEAR layer mixing is an important fluid physics phenomenon in scramjet combustors for hypersonic vehicles. CFD codes must be validated and calibrated so that designers have confidence in the computational results they are getting using them. One area of concern is the ability of CFD codes to adequately compute turbulent shear layer mixing, the main concern being the limitations imposed by turbulence models. This is vital since shear layer mixing rates can be a major design criterion for sizing of combustors.

The aim of this study is to compute three shear layer flows and compare the predictions with published results by Sullins.[1] In performing shear layer computations, the main objective is to predict shear layer growth, which is usually given in terms of a shear layer spreading rate $db/dx$. Most experimental data for $db/dx$ have been obtained for incompressible shear flows. Correlations have been developed for the data, but there is scatter of a factor of 2.[1] Data for compressible shear flows are very scarce; however, experimentalists have derived correlations similar to those for the incompressible ones. The experimental data scatter must be kept in mind when computational results do not match experimental results exactly. All the computational variables that can create error, such as grid resolution, numerical accuracy, and turbulence modeling, must not be emphasized more than errors caused by lack of information about the problem, such as experimental setup or exact inflow conditions, since such factors can also cause deviation of the computational result from the experimental one. Thus, fair judging of the accuracy of computational methods can be achieved only if the experiments are fully documented.

The USA-series code, used for the computations, enables a systematic study of the effect of turbulence modeling on the calculations, since there are three models available in the code. Sullins's experimental study covers a range of convective Mach numbers ($M_c$) between 0.25 and 0.5 in which compressibility effects are mild. None of the turbulence models, therefore, have explicit compressibility correction terms incorporated. A comparison between time-marched and space-marched solutions was also done since both options are available.

Received Oct. 15, 1990; revision received Feb. 8, 1991; accepted for publication Feb. 9, 1991. 

*Member, Technical Staff, 1049 Camino Dos Rios. Member AIAA.

## II. USA-Series Code

The code used for this shear layer study is a USA (unified solution algorithm)-series code.[2] This is a versatile set of codes that can be used to compute numerical solutions to a large variety of fluid dynamic problems by solving either the Euler or the Reynolds-averaged form of the Navier-Stokes equations (RANS) in two or three dimensions. They are constructed with a synergistic operational unification of many solution methodologies, both explicit (multistage Runge-Kutta) and implicit (approximate factorization and relaxation). The codes can be used in either a time-dependent or space-marching mode. A common discretization, up to third-order accurate, is built into these codes, based on the total variation diminishing (TVD) formulation for the convective terms within a finite-volume framework. This upwind formulation guarantees oscillation-free solutions while keeping the numerical dissipation to a minimum. For most viscous flow applications, this approach enables a faithful representation of the viscous diffusion with minimal contamination from artificial numerical dissipation. Several Riemann solvers are available for defining fluxes at cell faces, Roe's approximate solver being the one most commonly used. A multizone structured grid book-keeping approach is used to facilitate the treatment of complex geometric topologies. Turbulence modeling options include an algebraic modified Baldwin-Lomax model,[3] a one-equation $k - L$ model,[4] and a two-equation $k - \varepsilon$ model with near-wall treatment,[5] all incorporating Goldberg's treatment for separated flow regions.[3-5] The capability to solve perfect gas, frozen gas, equilibrium gas, and finite-rate reacting gas flows exists; the number of species and types of chemical reactions are arbitrary and user specifiable. The code permits flexible specification of point-wise boundary conditions, using either templates or user-coded subroutines.

## III. Computational Setup

The computational grid is set up with three zones as shown in Fig. 1. Zones 1 and 2 exist solely to allow the flow to develop boundary layers off the finite-thickness splitter plate trailing edge, thereby creating realistic inflow conditions into zone 3, which is the shear layer mixing region. While the experimental facility extended downstream to 35.5 in., most of the reported data ended at 13.07 in. Since the dominant part of the flow is supersonic, it is assumed that truncating the domain at 20.0 in. will not affect the results adversely. The upstream boundary conditions for zones 1 and 2 are the

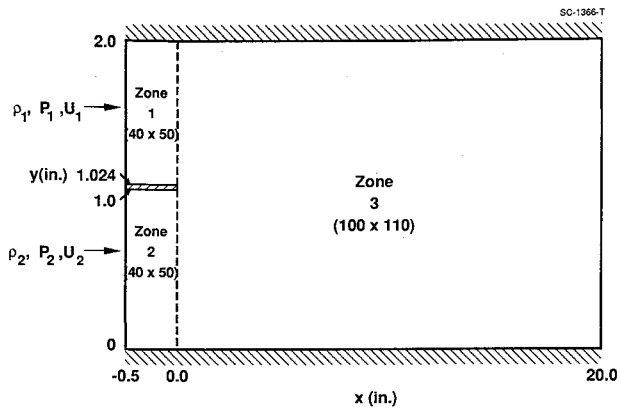


**Fig. 1 Computational setup of shear layer mixing.**

respective fixed flow conditions reported by Sullins,[1] the walls are assumed to be adiabatic, zonal continuity conditions are imposed between zones 1 and 3 and between zones 2 and 3, and the outflow of zone 3 is treated as a supersonic outflow boundary. Zones 1 and 2 have grids of 40 × 50 each and zone 3 has a grid of 100 × 110. The minimum spacing used at all walls is 0.00001 in.

Since the experimental flowfield was reported as two-dimensional, the shear layer computations were done using the two-dimensional perfect gas RANS mode with a specific heat ratio $\gamma = 1.4$.

## IV. Results

### A. Shear Layer Definition

In computing the shear layer spreading rate, Sullins[1] chose the following equations to define the spreading thickness $b$:

$$U_{\text{lower}} = 0.1(U_1 - U_2) + U_2 \tag{1}$$

$$U_{\text{upper}} = 0.9(U_1 - U_2) + U_2 \tag{2}$$

where the subscripts 1 and 2 refer to the low- and high-speed sides, respectively. With these definitions the spreading thickness is

$$b = y(\text{at}U_{\text{upper}}) - y(\text{at}U_{\text{lower}}) \tag{3}$$

and the spreading rate is

$$db/dx = (b_i - b_{i-1})/(x_i - x_{i-1}) \tag{4}$$

where subscripts $i$ and $i-1$ refer to successive streamwise $x$ stations at which data have been taken.

Sullins chose a specific $x$ station to get core values for $U_1$ and $U_2$ because the flow conditions were not measured right off the splitter plate edge; for the computation, however, $U_1$ and $U_2$ were taken from the fixed inflow conditions. This discrepancy is unavoidable since the exact inflow conditions, used in the experiment and needed for the computation, are not specified. The computation cannot use the core values that Sullins used since the core flows have evolved somewhat differently in experiment and computation. This difference is noted, and "experimental" spreading thicknesses and spreading rates have been calculated using the experimental $U$-velocity profiles with $U_1$ and $U_2$ taken from the computation. These results are presented as "graphical results" obtained from the experiment.

### B. Case 1

This case is set with the low- and high-speed flows at $M_1 = 1.0$ and $M_2 = 2.0$, respectively. The pressure ratio is $P_2/P_1 = 1.0078$, and the density ratio is $\rho_2/\rho_1 = 1.5116$ computed from plenum conditions of $P_{t1} = 1.03772 \times 10^5$ N/m$^2$, $P_{t2} = 4.3208 \times 10^5$ N/m$^2$, and $T_t = 283.3$ K. Core velocities are $U_1 = 309.1$ m/s and $U_2 = 504.7$ m/s; the reported core velocities measured at $x = 5.94$ in. are $U_1 = 291.7$ m/s and $U_2 = 502.9$ m/s. The sonic condition was chosen for the computation since the report states that the low-speed flow varied within a Mach number range of 0.8 to 1.2. One can see that even for $M_1 = 1$ the velocity $U_1$ is still high compared to the experimental value. This uncertainty points out a serious deficiency in validation of shear flow experiments: these should be set up so that the geometry from the plenum to the test section is provided, thus enabling the computation to start from the plenum. This would eliminate the uncertainty about the flow conditions to be applied at the splitter plate edge. By choosing $M_1 = 1.0$, a subsonic shear flow region is created, in agreement with the experimental observations, but the overexpanded jet condition reported[1] is not predicted.

The results for this case will now be discussed, bearing in mind the aforementioned uncertainties. Figures 2 and 3 show

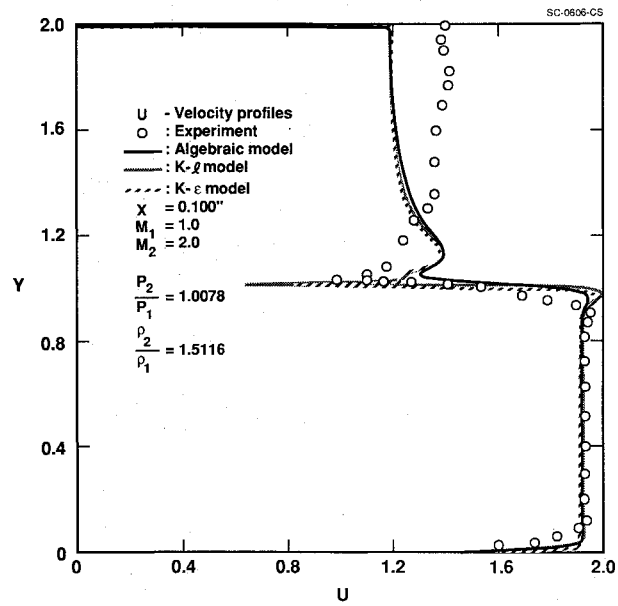


**Fig. 2 $U$-velocity profile at $x = 0.100$ in. for case 1. Turbulence model comparison.**

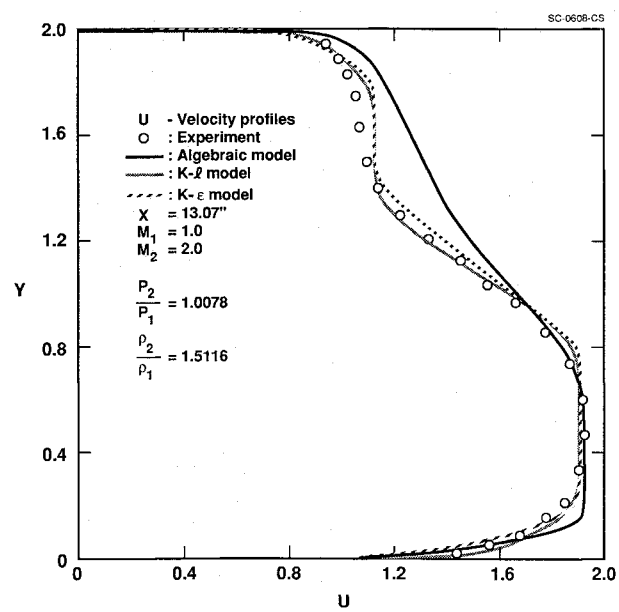


**Fig. 3 $U$-velocity profile at $x = 13.07$ in. for case 1. Turbulence model comparison.**

the $U$-velocity profiles at two $x$ stations downstream of the splitter plate. At $x = 0.1$ in., the discrepancy in the low-speed side flow conditions is observed, whereas those of the high-speed side match the experiments much better; at $x = 13.07$ in., the $U$-velocity profiles are in good agreement with the experimental data. The results using the algebraic turbulence model deviate from the experimental data the most; those using the $k - L$ and the $k - \varepsilon$ models are very similar and close to the experimental data. Figure 4 shows computed shear layer thickness $b$ at $x = 5.94$ in., and at $x = 13.07$ in.; the algebraic model predicts too large a shear layer thickness, whereas the predictions using the one- and two-equation models coincide with the experimental data. Table 1 summarizes the results for case 1.

The deviation of the $k - \varepsilon$ model prediction from the spreading rate based on the published $U$-velocity profiles is only 3%, which correlates with the degree of agreement seen in the $U$-velocity profile comparisons. As an independent check, Dimotakis's formula (Eq. (9) of Ref. 6) was also applied, yielding a value of 0.035 for the spreading rate, which is within 5% of the $k - \varepsilon$ model result.

### C. Case 2

This case has the low-speed flow set at $M_1 = 1.2$ and the high-speed flow at $M_2 = 2.0$. The pressure ratio is $P_2/P_1 = 0.9980$, and the density ratio is $\rho_2/\rho_1 = 1.3631$ computed from plenum conditions of $P_{t1} = 1.4627 \times 10^5$ N/m$^2$, $P_{t2} = 4.3510 \times 10^5$ N/m$^2$, and $T_t = 275.0$ K. Core velocities are $U_1 = 366.2$ m/s and $U_2 = 497.4$ m/s; the reported core velocities measured at $x = 2.18$ in. are $U_1 = 355.7$ m/s and $U_2 = 495.6$ m/s. Figures 5 and 6 show $U$-velocity profiles at two $x$ stations. The same trends as those mentioned for case 1 are evident for this case too: the algebraic model diffuses the shear layer too much and the $k - L$ and $k - \varepsilon$ models do quite well in following the shear layer. (There is no explanation given in Ref. 1 for the kink in the $U$-velocity profile evident at $x = 13.07$ in., Figure 7 shows the spreading thickness. Again, the same trends as in case 1 exist here. Table 2 summarizes the results for case 2.

It is noted that the experimentally deduced spreading rate is lower than that of case 1. It is also noted that all three turbulence models follow the trend of the data. Dimotakis's formula[6] predicts a spreading rate of 0.025, in agreement with both the $k - L$ and the $k - \varepsilon$ model predictions.

### D. Case 3

Here the low- and high-speed flows are at $M_1 = 1.25$ and $M_2 = 3.06$, respectively. The pressure ratio is $P_2/P_1 = 0.9096$, and the density ratio is $\rho_2/\rho_1 = 1.9574$ computed from plenum conditions of $P_{t1} = 1.3434 \times 10^5$ N/m$^2$, $P_{t2} = 1.8898 \times 10^6$

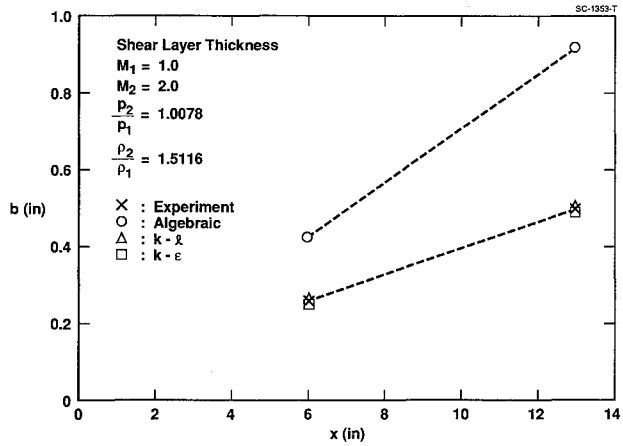


**Fig. 4 Shear layer spreading thickness $b$ for case 1. Turbulence model comparison.**

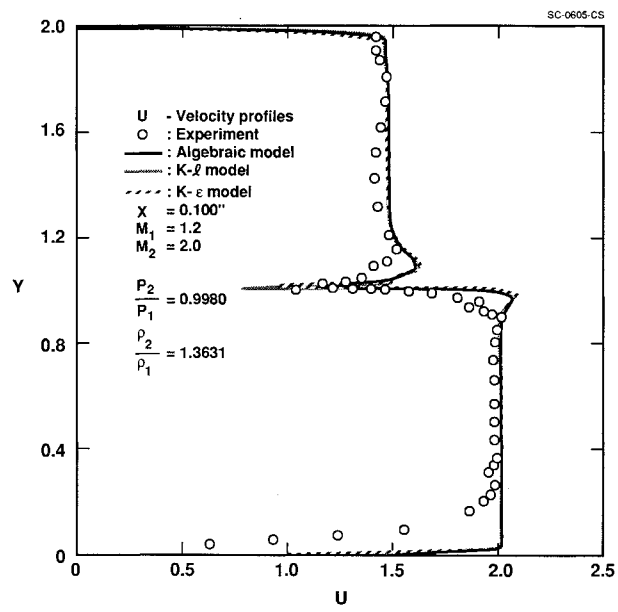


**Fig. 5 $U$-velocity profile at $x = 0.100$ in. for case 2. Turbulence model comparison.**

**Table 1 Computed and experimental spreading rate data**

| Case 1 | Algebraic | $k - L$ | $k - \varepsilon$ | Exp. (publ.) | Exp. (graph) |
|---|---|---|---|---|---|
| $b$ ($x = 5.94$ in.) | 0.43 | 0.25 | 0.24 | 0.26 | 0.25 |
| $b$ ($x = 13.07$ in.) | 0.92 | 0.48 | 0.50 | 0.57 | 0.52 |
| $db/dx$ (in./in.) | 0.069 | 0.032 | 0.037 | 0.044 | 0.038 |
| % error (publ.) | 57 | −27 | −16 | — | — |
| % error (graph) | 82 | −16 | −3 | — | — |

**Table 2 Computed and experimental spreading rate data**

| Case 2 | Algebraic | $k - L$ | $k - \varepsilon$ | Exp. (publ.) | Exp. (graph) |
|---|---|---|---|---|---|
| $b$ ($x = 2.18$ in.) | 0.07 | 0.09 | 0.08 | — | 0.11 |
| $b$ ($x = 5.94$ in.) | 0.32 | 0.19 | 0.17 | — | 0.24 |
| $b$ ($x = 13.07$ in.) | 0.77 | 0.37 | 0.35 | — | 0.40 |
| $db/dx$ (5.94 − 2.18) | 0.065 | 0.028 | 0.025 | — | 0.035 |
| $db/dx$ (13.07 − 5.94) | 0.063 | 0.025 | 0.025 | 0.027 | 0.022 |
| % error (publ.) | 133 | −7 | −7 | — | — |
| % error (graph) | 186 | 14 | 14 | — | — |

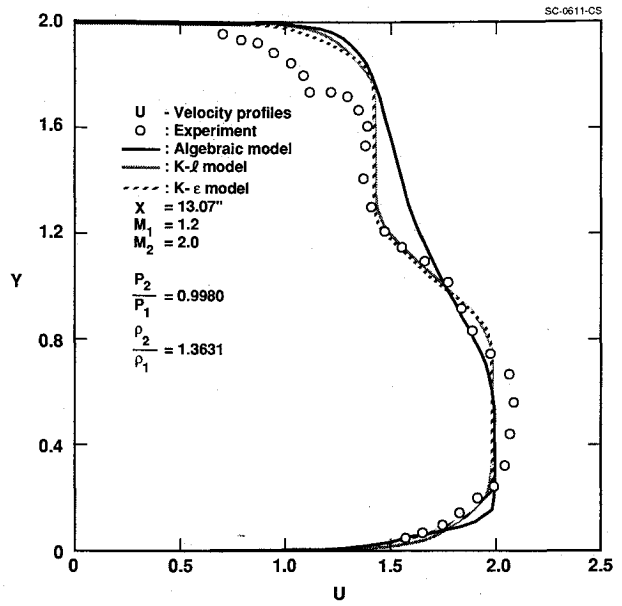


Fig. 6 *U*-velocity profile at $x = 13.07$ in. for case 2. Turbulence model comparison.

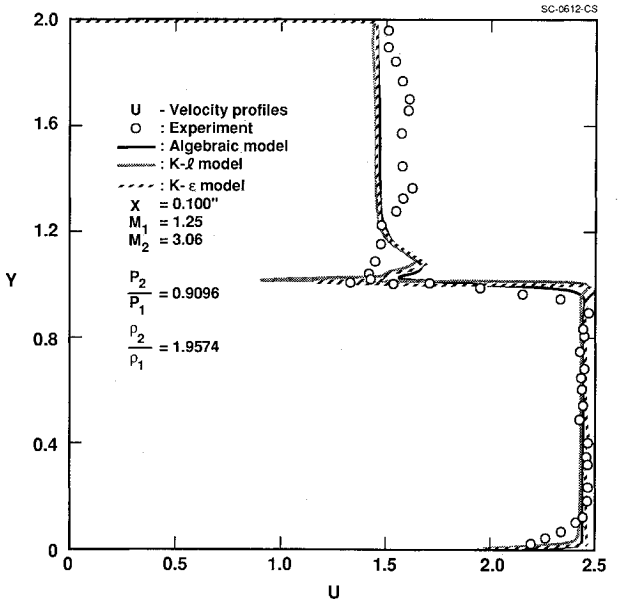


Fig. 8 *U*-velocity profile at $x = 0.100$ in. for case 3. Turbulence model comparison.

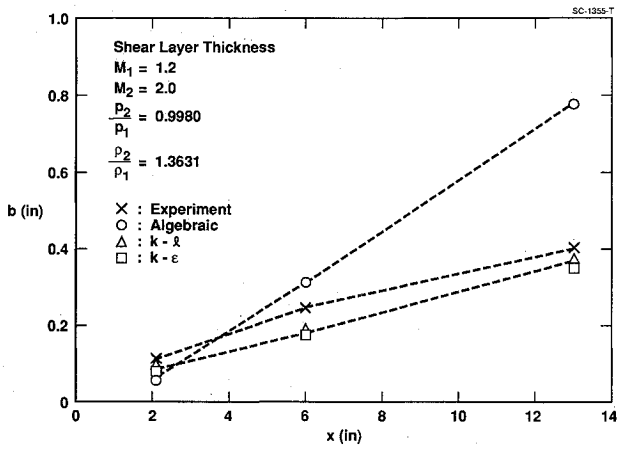


Fig. 7 Shear layer spreading thickness *b* for case 2. Turbulence model comparison.

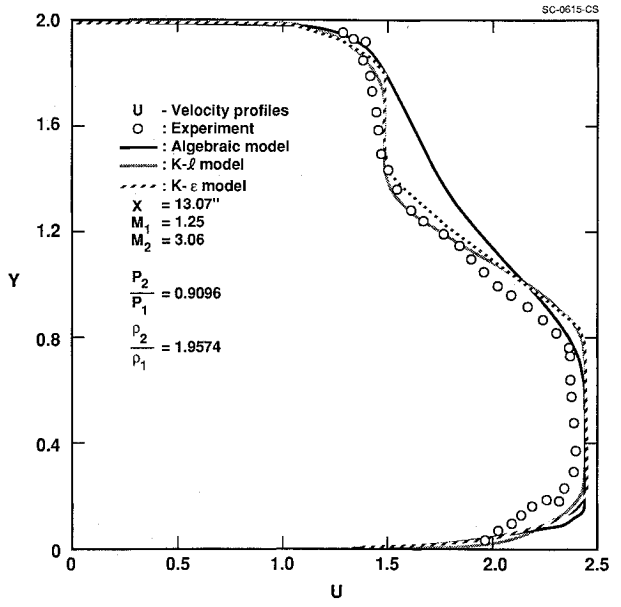


Fig. 9 *U*-velocity profile at $x = 13.07$ in. for case 3. Turbulence model comparison.

N/m$^2$, and $T_t = 294.9$ K. Core velocities are $U_1 = 376.9$ m/s and $U_2 = 628.1$ m/s; the reported core velocities measured at $x = 2.18$ in. are $U_1 = 376.4$ m/s and $U_2 = 624.4$ m/s. This case is at a higher Mach number to check Mach number effect on shear layer spreading rates. Figures 8 and 9 show *U*-velocity profile data at the same *x* stations as before. The trends observed in cases 1 and 2 are evident here too: the algebraic model diffuses the shear layer too much, while the $k - L$ and $k - \varepsilon$ models enable correct prediction of the shear layer development. As in case 2, the experimental data show flow structures which are not predicted by the computations; this is most evident at $x = 13.07$ in. Figure 10 shows the spreading thickness. Once again, the same trends as in cases 1 and 2 exist here. Table 3 is a summary of the results for case 3.

It is noted that, unlike the previous cases, the experimentally deduced spreading rate increased between the two meas-

Table 3 Computed and experimental spreading rate data

| Case 3 | Algebraic | $k - L$ | $k - \varepsilon$ | Exp. (publ.) | Exp. (graph) |
|---|---|---|---|---|---|
| $b$ ($x = 2.18$ in.) | 0.17 | 0.13 | 0.13 | — | 0.15 |
| $b$ ($x = 5.94$ in.) | 0.39 | 0.29 | 0.24 | — | 0.23 |
| $b$ ($x = 13.07$ in.) | 0.91 | 0.46 | 0.55 | — | 0.57 |
| $db/dx$ (5.94 − 2.18) | 0.059 | 0.042 | 0.030 | 0.030 | 0.021 |
| $db/dx$ (13.07 − 5.94) | 0.072 | 0.024 | 0.043 | 0.040 | 0.048 |
| % error (publ.) | 80 | −40 | 7.5 | — | — |
| % error (graph) | 50 | −50 | −10 | — | — |

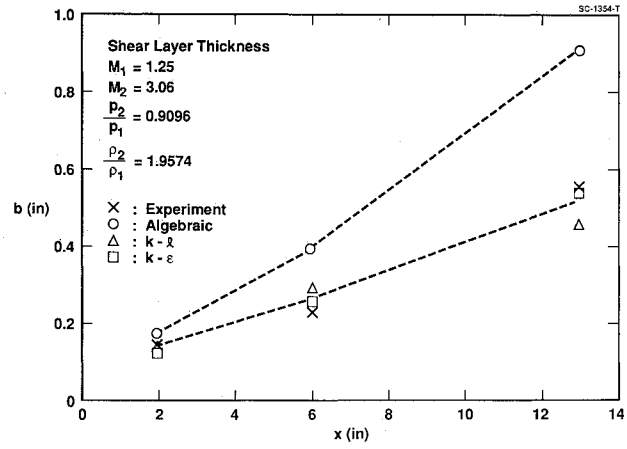


**Fig. 10 Shear layer spreading thickness $b$ for case 3. Turbulence model comparison.**

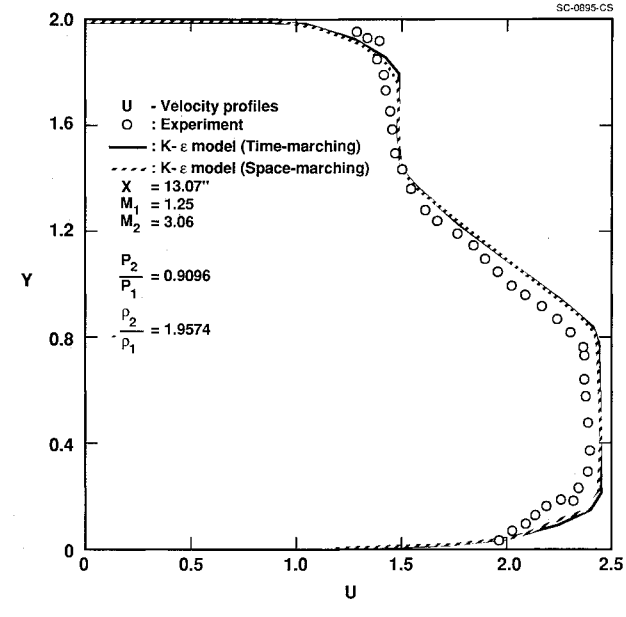


**Fig. 11 $U$-velocity profile at $x = 13.07$ in. for case 3. Space-marching vs time-marching comparison.**

urements. The results using the algebraic and the $k - \varepsilon$ models follow this trend, whereas the one using the $k - L$ model does not. Spreading rate errors have remained small with the $k - \varepsilon$ model, however, both the algebraic and the $k - L$ models created relatively large spreading rate errors in this case. Dimotakis's formula predicts $db/dx = 0.035$, 19% below the $k - \varepsilon$ prediction.

A space-marched solution was also obtained for case 3 using the $k - \varepsilon$ turbulence model. The results at all stations are essentially the same as those of the time-marched computations. Figure 11 shows the comparison at $x = 13.07$ in.

## V. Conclusions

Compressible shear layer flows need to be validated computationally since the design of scramjet combustors, in which such flows occur, will rely heavily on computational techniques.

In the present work, turbulent supersonic shear layer mixing with mild compressibility effects was computed using a USA-series code. Three shear layer cases were shown, using three turbulence models each: 1) algebraic, 2) one-equation $k - L$, and 3) two-equation $k - \varepsilon$ model. The solutions using the one- and two-equation models match the experimental $U$-velocity profiles better than those using the algebraic model. Shear layer thicknesses and shear layer spreading rates also compare well with the experimental data especially with the $k - \varepsilon$ model, leading to the conclusion that the $k - \varepsilon$ turbulence model outperforms the algebraic and the $k - L$ models for free shear mixing flows. This indicates the strength of point-wise models for such flows. Another observation is that the algebraic turbulence model consistently diffuses the shear layer too much; however, all trends are predicted correctly with this model. The general conclusion is that higher order models outperform algebraic ones in predicting free shear flows. The space-marched and time-marched solutions for case 3 are practically the same, indicating that space-marching methods might be adequate for supersonic shear flows. More studies need to be done to gain confidence in and understanding of the ability of computational methods to predict free shear layer flows. Last but not least, experimentalists must make an effort to provide all the details necessary for a proper setup of a RANS computation aimed at predicting their data.

## References

[1]Sullins, G. A., "Shear Layer Mixing Tests," NASP Contractor Report 1053, July 1989.

[2]Chakravarthy, S. R., and Szema, K.-Y., "Unified 'Nose-to-Tail' Computational Method for Hypersonic Vehicle Applications," AIAA Paper 88-2564, 1988.

[3]Ramakrishnan, S. V., and Goldberg, U. C., "Versatility of an Algebraic Backflow Turbulence Model," AIAA Paper 90-1485, 1990.

[4]Goldberg, U. C., and Chakravarthy, S. R., "Separated Flow Predictions Using a Hybrid $k - L$/Backflow Model," *AIAA Journal*, Vol. 28, No. 6, June 1990, pp. 1005–1009.

[5]Goldberg, U. C., and Ota, D. K., "A $k - \varepsilon$ Near-Wall Formulation for Separated Flows," AIAA Paper 90-1482, 1990.

[6]Dimotakis, P. E., "Turbulent Free Shear Layer Mixing," AIAA Paper 89-0262, 1989.